

Microstructure and Fracture Toughness of Gadolinium Aluminates Synthesized via Reverse Chemical Precipitation

W. Hernández Muñoz¹, J. Serrato Rodríguez², J. Muñoz Saldaña²,
J. Zárate Medina¹

¹ Instituto de Investigación en Metalurgia y Materiales, Universidad Michoacana de San Nicolás de Hidalgo, Mexico

² Cinvestav Unidad Querétaro, Mexico

Abstract: Gadolinium aluminate (GAO) was prepared by reverse chemical precipitation out of reagent grade chemical salt precursors i.e. gadolinium oxide and aluminum sulphate derived pseudoboehmite. The obtained gel like precipitates were dried, and calcined at various temperatures. Powders were uniaxially pressed into compacts and sintered in air up to 1600°C. Calcined and sintered compacts were characterized by XRD, FESEM, HRTEM, Raman spectroscopy, Arquimedes density measurements, Vickers indentation micro hardness, and fracture toughness (K_{IC}) from crack indented specimens. Compacts were sintered up to 98.3±3.3 % high density values. Gadolinium aluminate perovskite $GdAlO_3$ phase (GAP) was mainly found throughout all the processing and sintering cycle, however a monoclinic low strength gadolinium aluminate, $Gd_4Al_2O_9$ (GAM) impurity phase was steadily found to be present despite tight stoichiometric and processing control. Such impurity phase was found to lower the fracture toughness down to $0.12\pm 0.01 \text{ MPa}\cdot\text{m}^{1/2}$.

Keywords: Reverse, chemical, precipitation, gadolinium aluminates.

I. Introduction

Rare earth based perovskite type oxides have been subject to research due to its optical, electrical, electronic, magnetic and structural properties for applications such as scintillator, phosphorescent, solid-state lasers, color TV monitors, fluorescent lamps, regenerator material for sub-4K cryo-coolers and radiation detectors [1–4]. Moreover perovskite-type ceramics exhibit low thermal conductivities which makes them attractive candidates for thermal barrier coatings (TBC) applications [5,6]. Gadolinium aluminate, (GAO) that belongs to such group has well studied properties [7,8], nevertheless there is scarce information about mechanical strength and fracture toughness as related to TBC [6].

GAO synthesis is normally carried out by two groups of techniques: solid-state reaction and wet-chemical methods [1,2,9,10]. Usually in the solid state route substantial mechanical mixing and prolonged heat treatments are required [2,11]. Many wet-chemical techniques such as the polymerized complex approach, combustion synthesis and sol-gel have been widely used. The latter techniques rely on costly analytical grade precursors, so the quest for an alternative source may be advantageous.

In the natural dropping non reverse approach a precipitate agent (usually ammonium hydrate) is added to a mixture solution that contains aluminum precursors, on the contrary the reverse dropping procedure involves adding the solution to a precipitate agent; the main difference between these two methods is that the non-reverse method starts with an acidic environment that will eventually change to basic, whereas in the reverse procedure basic pH is maintained constant; these different environments can modify the hydrolysis-complex processes, thus variations in morphology and particle size, crystalline phase and chemical composition of the precipitates can occur [12].

In the present work a new approach to the synthesis of gadolinium aluminate consists on the use of the pseudoboehmite (PB) as a low-cost aluminate precursory phase, that can be easily dispersed in order to obtain non agglomerated highly reactive nanometric particles. PB can be readily synthesized by desulfation of reagent grade or even through the low cost aluminum sulfate using ammonia solution. In both cases, it has been proved, through the actual lanthanum aluminate synthesis and characterization, that products are free of contaminants [13]. GAO powders obtained through reverse precipitation were submitted to heat treatment and structurally characterized by XRD, FESEM, HRTEM and Raman spectroscopy. Finally, the synthesized GAO powder was pressed and sintered into compacts to further characterize hardness and fracture toughness via conventional ceramic methods. It is hoped that the present results will be useful considering the scarce data currently available in the literature.

II. Materials And Methods

A flow chart of the process for preparing GAO powders is shown in Fig.1. PB was synthesized by chemical precipitation, in which, reactive grade aluminum sulphate (Meyer 99.9 %) was dissolved in distilled water (300g/L) followed by stirring for 24 h and then filtered to form the initial solution. Subsequently, ammonium hydroxide (J.T Baker 68%) which was previously heated (60°C) was added to the initial solution at a rate of 0.1 mL/min and stirred; Additional ammonium hydroxide was added in order to keep pH above 11.

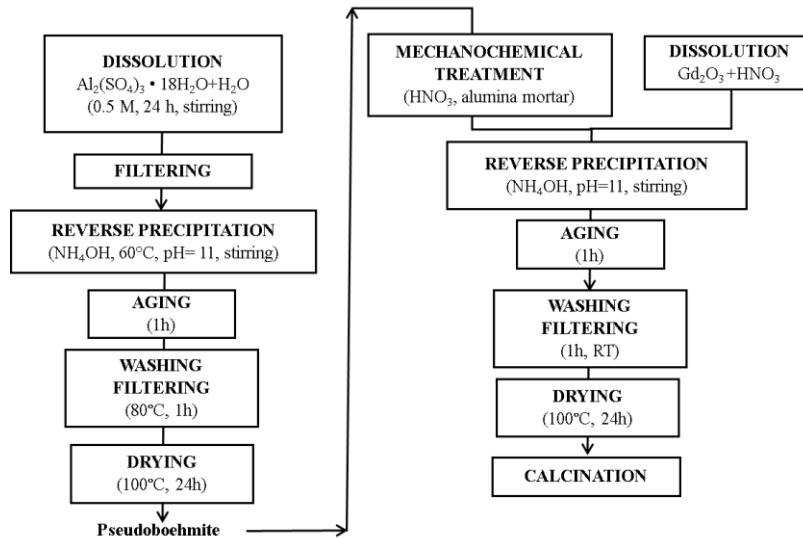


Figure 1. Flow chart for the preparation of GAO powders.

After completion of precipitation reaction, gel-like precipitates were obtained, then precipitates were aged and stirred for 1 h, followed by filtering and washing with deionized water at 60°C many times until no gel formation was observed when some drops collected from last filtration were dropped on barium chloride. Gels were dried at 80°C for 24 h. After that powders were milled in an alumina mortar.

0.5 M solution of gadolinium oxide (Alpha Aesar 99%) was mixed with nitric acid (Meyer 70%), separately PB was peptized by adding nitric acid while it was milled manually in an alumina mortar. Both gadolinium oxide solution and peptized PB were mixed and stirred, then ammonium hydroxide was dropped maintaining pH above 11 producing gel-like precipitates. The suspension was stirred for 1 h, washed in distilled water and filtered. Filtered gels were dried at 100°C for 24 h to render the GAO precursor. Calcination was carried out at different temperature and 5 h. The calcined powders were uniaxially pressed at 550 MPa and sintered at 1600°C for 5 h to form disc-like 11x1.2 mm compacts.

DRX spectra were collected in Bruker D8 Advance spectrometer using Cu K α radiation, SEM and TEM examination were conducted in a JEOL 6400 microscope and Philips Technai F-20, respectively. Raman spectra was recorded in a Bruker Senterra using 532 nm laser. Density measurements were done by the Archimedes method.

Fracture toughness (K_{IC}) was assessed from equation (1)[14]:

$$K_{IC} = 0.016 232H_v a c^{-3/2} \quad (1)$$

where “H_v” is the hardness, “a” is the half length of the indent diagonal, “c” is the half- crack length measured from the middle of the indent to the tip of the crack .

III. Results

Figure 2 shows XRD spectra of biphasic monoclinic (GAM) and orthorhombic gadolinium aluminate (GAP) powders calcined at different temperatures for 5 hrs. At 800°C few poorly defined diffraction peaks are observed indicating that powders are amorphous. At 900°C, the sole monoclinic well crystallized phase firstly appears (JCPDS 00-046-0396). The orthorhombic phase (JCPDS 00-046-0395) develops at 1000°C. As temperature rises up to 1400 °C the GAP phase increases its crystallinity, while the GAM phase tends to disappear within the 1000-1400°C temperature range. The 1600°C reactive sintering temperature however, reveals the GAP to GAM partial conversion, pointing to the high instability of such phases. Fig. 3 refers to the GAP GAM congruently and incongruently melting phase nature and point to its chemical GAP to GAM interchangeability via the reaction: GdAlO₃→ Gd₄Al₂O₉ + Al₂O₃.

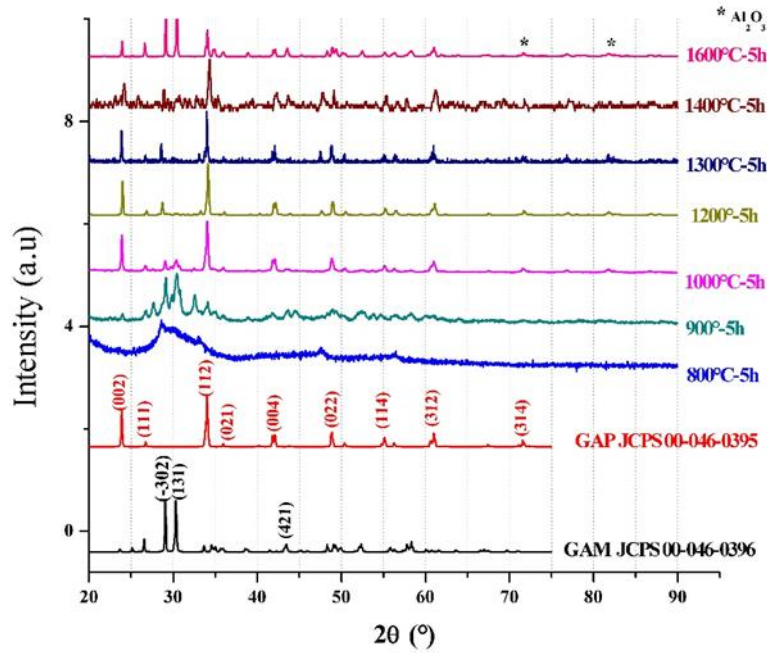


Figure 2. XRD spectra of GAO powders calcined at different temperatures.

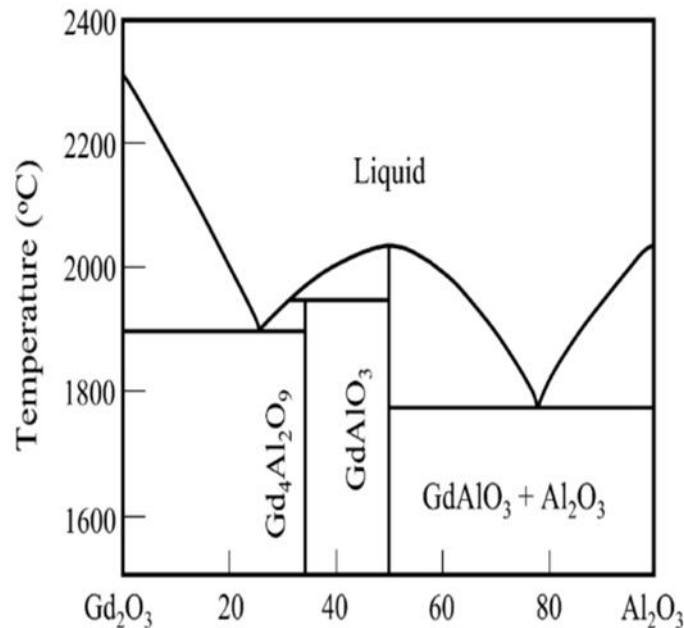


Figure 3. Phase diagram of Gd_2O_3 - Al_2O_3 system [15].

Fig.4 is the Raman spectra for the GAM phase at 900°C, also, evidencing small amounts of the GAP phase; the second spectra shows the GAP phase at 1400°C and small amounts of the GAM phase. Raman results were comparable to those of Chopelas et al. [16] and Bagnato[17], finding 24 Raman modes for gadolinium aluminate i.e. $7A_g+7B_1g+5B_2g+5B_3g$. The spectra in figure 4 depicts the following frequencies: A_g (95 cm^{-1} , 146 cm^{-1} , 232 cm^{-1} , 313 cm^{-1} , 368 cm^{-1}), B_g (111 cm^{-1} , 222 cm^{-1} , 405 cm^{-1} , 414 cm^{-1}) and B_3g (174 cm^{-1} , 551 cm^{-1}). Raman modes fit in three categories: oxygen stretching in AlO_6 octahedron (highest energy modes at $500\text{--}600\text{ cm}^{-1}$), oxygen bending in AlO_6 octahedron ($300\text{--}450\text{ cm}^{-1}$), and rotation and translation for the Gd cation ($<300\text{ cm}^{-1}$) [16,18]. The remaining smaller bands in figure 4 at 88 cm^{-1} , 345 cm^{-1} and 381 cm^{-1} belong to the GAM phase.

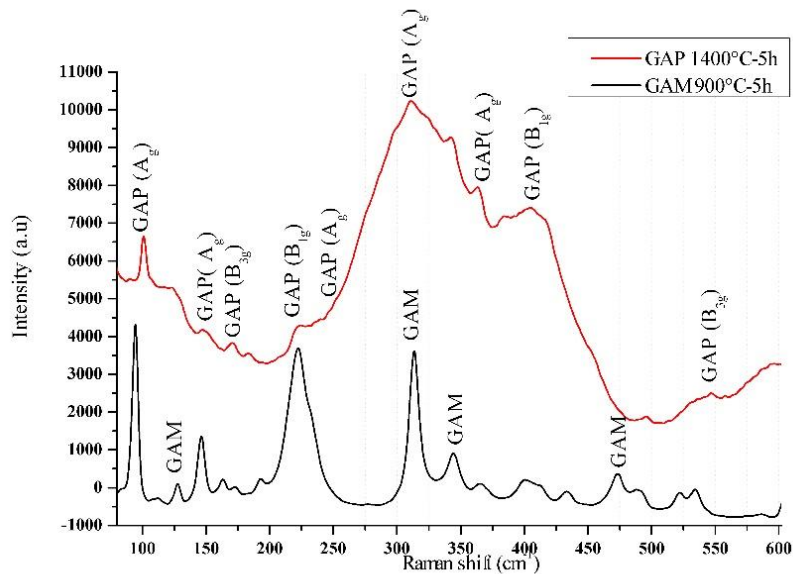


Figure 4. Raman spectra of GAO powders calcined at 900°C and 1400°C for 5h.

Fig. 5(a) is a FESEM secondary electrons micrograph of micron size powders after being calcined at 1400°C for 5 h. GAP, GAM phases can be sort out by EDX, and through both morphology and atomic mass contrast differences. The gray GAP phase with straight grain boundaries and well-formed orthorhombic crystals at the background are resolved within the lighter anhedral rounded grain boundaries GAM phase. Fig. 5(b) shows a FESEM micrograph of a 1600°C sintered pellet that was uniaxially pressed; the predominantly gray GAP phase appears on most of the picture, and the light contours correspond to the transforming GAM phase. There is also evidence by SEM and X-ray diffraction of the formation of small amounts of alumina phase.

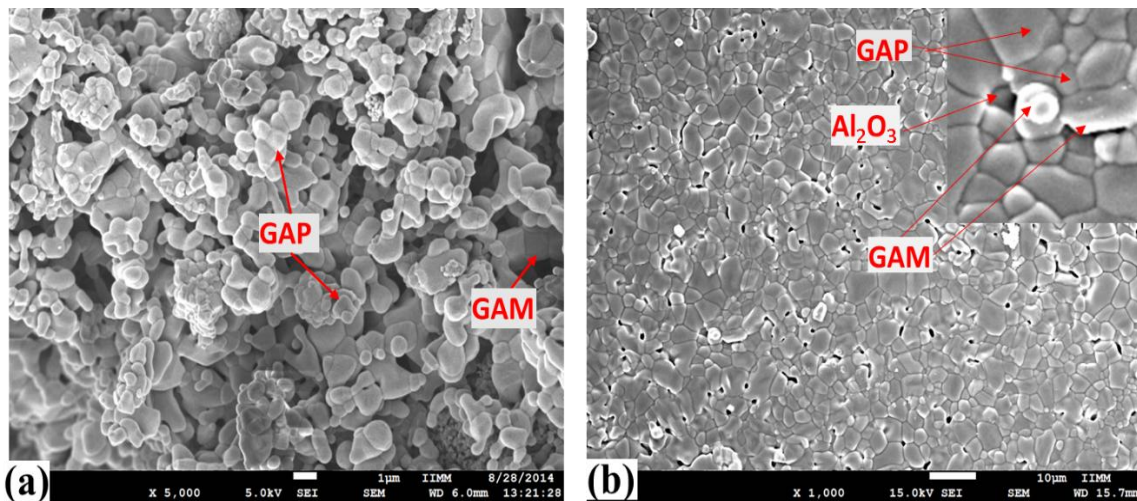


Figure 5. FESEM secondary electrons micrographs of powders calcined at 1400°C for 5 h (a) and sintered at 1600°C (b).

Fig. 6 is a HRTEM micrograph of the GAM phase growing on the contours of the larger GAP phase. The measured fringe spacing in IFFT inserts of both phases, point to the (240), (223), (331) planes of the GAP phase (JCPDS 00-046-0395); and the (245) plane of the GAM (JCPDS 00-946-0395) phase. The disordered planes of the GAM phase may be a pointer to low crystallinity, and distinctly contrast with the GAP reticular sharp crystalline planes.

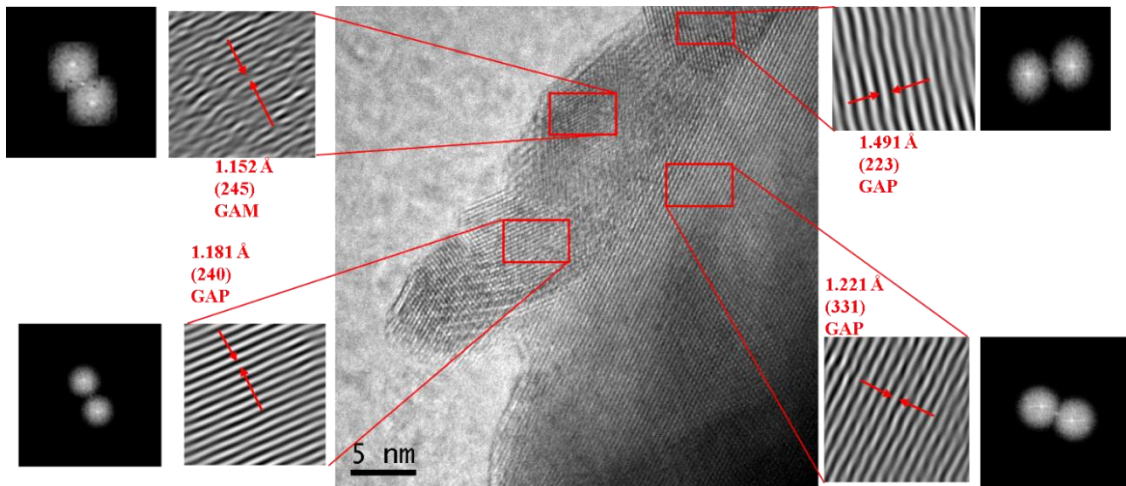


Figure 6. HRTEM micrograph of GAO powders calcined at 1400°C.

Fig. 7a SEM micrograph illustrates a Vickers indentation on a sintered polished section and the resulting cracks that are used to work out fracture toughness. Fig. 7b SEM shows a crack path propagation through the smaller grain sized weaker GAM phase. Crack propagates preferentially through the weaker GAM phase and goes round the GAP stronger phase. A typical value of the micro hardness is 1.45 ± 0.14 GPa and the work out fracture toughness is 0.12 ± 0.01 MPa.m^{1/2} as measured from an average of indentation twelve fields of view.

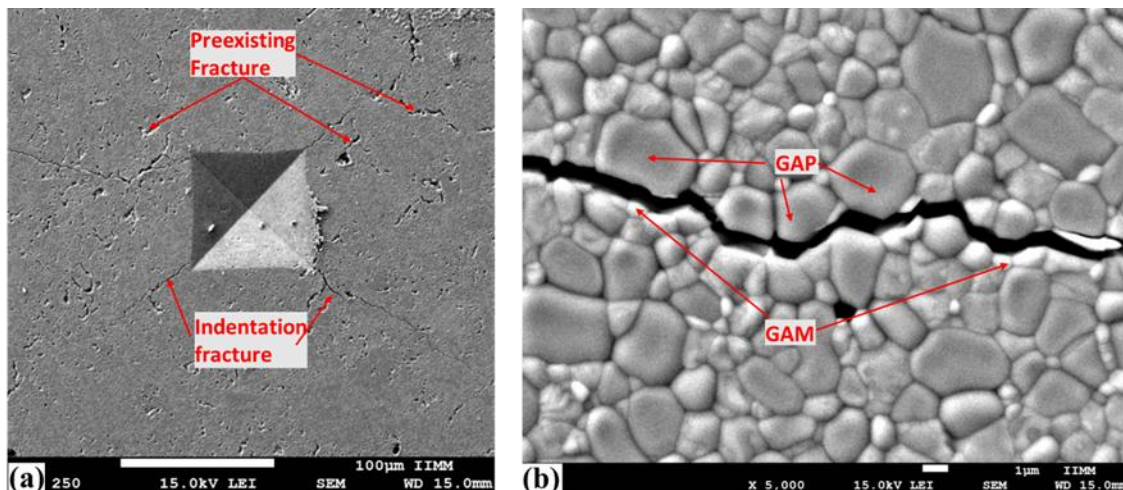


Figure 7. SEM micrographs of Vickers indentation (a) and crack path propagation on polished surface.

IV. Discussion

The reverse precipitation synthesis procedure followed here, consisting of adding the solution to a precipitate agent while pH is kept constant, allowed for an instantaneous precipitation of pure, highly reactive gadolinium aluminates. Swift experimental reaction conditions were set up to avoid segregation of Gd and Al phases during precipitation that could lead to the formation of other aluminate types [10]. The reverse precipitation synthesis allows a smooth aluminate formation routine and a higher PB reactivity presumably brought about through nano-metric diffusion paths as described elsewhere for lanthanum aluminates [19]. As found in the present approach, GAM and GAP simultaneously occur as in other synthesis techniques, e.g. sol-gel and chlorides (Gd, Al) precursors detected GAP, GAM and Al₂O₃ after calcination at 1000°C and, small amounts of GAM were found when GAP was synthesized by solid-state reaction [18,20].

As shown by X-ray diffraction, as synthesized powders are amorphous and when calcined present phase transformation from amorphous to the monoclinic (GAM) at 900°C, and to the GAP phase up to 1400°C, which is also seen by Raman spectroscopy. Raman identified frequency modes are oxygen stretching and oxygen bending. Therefore, gadolinium aluminate crystalline structure may have a distortion since bonding angles are more affected than interatomic distances as discussed by Bagnato [17].

Reaction sintering was found at 1600°C, where the majority GAP phase presumably undergoes the reaction: $4\text{GdAlO}_3 \rightarrow \text{Gd}_4\text{Al}_2\text{O}_9 + \text{Al}_2\text{O}_3$, that results on the formation of the GAM and alumina phases within the microstructure. GAM grows adjacent to GAP and the alumina and porosity by-product phases, lay alongside the grain boundaries as found by the FESEM and HRTEM study. The resulting multiphase material, though dense may not be expected to be tough. The fired density of the compact is high, $98.3 \pm 3.3\%$, compared to Sinha [9] who reported 95% at the 1700°C higher sintering temperature. The fracture toughness however, is rather low, $0.12 \pm 0.01 \text{ MPa} \cdot \text{m}^{1/2}$ weigh against $1.87 \text{ MPa} \cdot \text{m}^{1/2}$ reported by Sharma [1] for the GAP phase. It was experimentally observed that fracture propagates through the GAM phase which is weaker and less crystalline than the GAP phase and therefore may behave as a stress concentrator that considerably decreases fracture toughness. Furthermore, it will also be seen by the micrographs, that preexisting cracks are present, that may be the result of the thermal expansion mismatch of the coexisting GAM, GAP phases.

V. Conclusion

The present approach to the synthesis of gadolinium aluminate based on the use of the pseudoboehmite (PB) as a low-cost aluminate precursory phase, leads to the formation of non-agglomerated highly reactive nanometric particles. Reaction sintering was found at 1600°C, where the majority GAP phase presumably undergoes the reaction: $4\text{GdAlO}_3 \rightarrow \text{Gd}_4\text{Al}_2\text{O}_9 + \text{Al}_2\text{O}_3$, that results on the formation of the GAM and small amounts of alumina and porosity phases within the microstructure. This multiphase material, though highly dense, presents low fracture toughness derived by the GAM phase that concentrates the stress.

Acknowledgements

This work was supported by the project CONACYT 177912 and CIC-UMSNH 12937.

REFERENCES

- [1]. A. Sinha, B.P. Sharma, P. Gopalan, H. Näfe, Study on phase evolution of $\text{GdAl}_{1-x}\text{Ga}_x\text{O}_3$ system, *J. Alloys Compd.* 492 (2010) 325–330.
- [2]. S. Cizauskaite, V. Reichlova, G. Nenartaviciene, a. Beganskiene, J. Pinkas, a. Kareiva, Sol–gel preparation and characterization of gadolinium aluminate, *Mater. Chem. Phys.* 102 (2007) 105–110.
- [3]. X. Dong, X. Cui, Z. Fu, S. Zhou, S. Zhang, Z. Dai, Study on preparation and luminescent properties of Eu^{3+} -doped LaAlO_3 and GdAlO_3 , *Mater. Res. Bull.* 47 (2012) 212–216.
- [4]. G. Suresh, G. Seenivasan, M.V. Krishnaiah, P. Srirama Murti, Investigation of the thermal conductivity of selected compounds of gadolinium and lanthanum, *J. Nucl. Mater.* 249 (1997) 259–261.
- [5]. R. Vaßen, M. Jarligo, T. Steinke, Overview on advanced thermal barrier coatings, *Surf. Coatings* 205 (2010) 938–942.
- [6]. D.R. Clarke, M. Oechsner, N.P. Padture, Thermal-barrier coatings for more efficient gas-turbine engines, *MRS Bull.* 37 (2012) 891–898.
- [7]. A. Sinha, B.P. Sharma, P. Gopalan, Development of novel perovskite based oxide ion conductor, *Electrochim. Acta.* 51 (2006) 1184–1193.
- [8]. R.K. Tamrakar, K. Upadhyay, D.P. Bisen, Variation in luminescence behavior of Yb^{3+} doped GdAlO_3 phosphor with gradual increase in Yb^{3+} concentration, *Infrared Phys. Technol.* 75 (2016) 160–167.
- [9]. A. Sinha, S.R. Nair, P.K. Sinha, Single step synthesis of GdAlO_3 powder, *J. Alloys Compd.* 509 (2011) 4774–4780.
- [10]. S. Chaudhury, S.C. Parida, K.T. Pillai, K.D. Singh Mudher, High-temperature X-ray diffraction and specific heat studies on GdAlO_3 , $\text{Gd}_3\text{Al}_5\text{O}_{12}$ and $\text{Gd}_4\text{Al}_2\text{O}_9$, *J. Solid State Chem.* 180 (2007) 2393–2399.
- [11]. A. Sinha, B.P. Sharma, H. Näfe, P. Gopalan, Synthesis of gadolinium aluminate powder through citrate gel route, *J. Alloys Compd.* 502 (2010) 396–400.
- [12]. H. Chen, Y. Gao, Y. Liu, H. Luo, Coprecipitation synthesis and thermal conductivity of $\text{La}_2\text{Zr}_2\text{O}_7$, *J. Alloys Compd.* 480 (2009) 843–848.
- [13]. J. Zárate, G. Rosas, P. P, Estructural transformations of the pseudoboehmite alumina to α -alumina, *Adv. Technol. Mater. Mater. Process.* 7 (2005) 181–186.
- [14]. L. Guo, M. Li, Y. Zhang, F. Ye, Improved Toughness and Thermal Expansion of Non-stoichiometry $\text{Gd}_{2-x}\text{Zr}_2 + x\text{O}_7 + x/2$ Ceramics for Thermal Barrier Coating Application, *J. Mater. Sci. Technol.* 32 (2016) 28–33.
- [15]. S. Sun, Q. Xu, Compound Powder Prepared by Co-Precipitation Method, *Key Eng. Mater.* 512–515 (2012) 535–538.
- [16]. A. Chopelas, Single-crystal Raman spectra of YAlO_3 and GdAlO_3 : Comparison to several orthorhombic ABO₃ perovskites, *Phys. Chem. Miner.* 38 (2011) 709–726.

- [17]. V. Bagnato, *Espectroscopia no infravermelho e Raman do aluminato de gadolínio puro e dopado com íons de terras raras*, master thesis, Universidade de São Paulo, São Paulo, 1983.
- [18]. G. Gouadec, P. Colomban, N. Piquet, M.F. Trichet, L. Mazerolles, Raman/Cr³⁺ fluorescence mapping of a melt-grown Al₂O₃/GdAlO₃ eutectic, *J. Eur. Ceram. Soc.* 25 (2005) 1447–1453.
- [19]. W. Hernández Muñoz, J. Serrato Rodríguez, J. Muñoz Saldaña, J. Zárate Medina, Synthesis of lanthanum aluminate by reverse chemical precipitation using pseudoboehmite as alumina precursor, *Appl. Radiat. Isot.* (2016).
- [20]. L. Luo, Z. Xiong, N. Zhou, Synthesis of gadolinium aluminate thin film by ion beam sputtering sequential deposition, *J. Rare Earths.* 28 (2010) 91–96.